iForest
Biogeosciences and Forestry

Research Article
doi: 10.3832/ifor4720-018
vol. 18, pp. 357-365

Classification of xeric scrub forest species using machine learning and optical and LiDAR drone data capture

Adrián Hernández-Ramos [1-2],
José René Valdez-Lazalde [1],
Héctor Manuel de los Santos-Posadas [1],
Valentín José Reyes-Hernández [1],
Pablito Marcelo López-Serrano [3],
Antonio Cano-Pineda [2],
Héctor Flores-Magdaleno [4]

Arid and semi-arid forest ecosystems represent the largest biomes on Earth. However, research on identifying their species using remote sensing techniques is still limited. Understanding the spatial distribution of vegetation is crucial for precision management. This can be achieved through methods that allow for the individual identification and classification of species, which are essential for accurately estimating forest inventory. The objective of this study was to identify and classify forest species present in a xeric shrubland (arid and semi-arid region) based on multispectral images, red-green-blue (RGB) images, and Light Detection and Ranging (LiDAR) data. All images and data were drone-captured. Machine learning algorithms such as Adaptive boosting (AB), Gradient boosting machine (GBM), Xtreme gradient boosting (XGB), Classification and regression trees (CART), Random Forest (RF), and Support vector machines (SVM) were employed. RF yielded better results for species and shrub class classification, with an accuracy of 0.64 and a Kappa coefficient of 0.56. Classification accuracy values per species were 0.73 (*E. antisyphilitica*), 0.70 (opuntias), 0.67 (palms), 0.65 (*L. tridentata*), 0.59 (trees and shrubs), and 0.55 (*A. lechuguilla*), all of which were obtained by combining the three types of data used. Spectral variables contributed the most metrics, followed by LiDAR and RGB. The results support the adoption of remote drone-mounted sensing systems for characterizing the complex forest vegetation in arid and semi-arid regions, thereby providing a decision-support tool for its management.

Keywords: Arid/semi-arid Ecosystem, Multispectral, Non-timber Forest Management, Remote Sensing

(1) Postgrado en Ciencias Forestales, Colegio de Postgraduados, Campus Montecillo (México); (2) Instituto Nacional de Investigaciones Forestales, Agrícolas y Pecuarias - INIFAP, Campo Experimental Saltillo, Saltillo, Coahuila (México); (3) Instituto de Silvicultura e Industria de la Madera, Universidad Juárez del Estado de Durango, Durango (México); (4) Postgrado en Hidrociencias, Colegio de Postgraduados Campus Montecillo (México)

@ José René Valdez-Lazalde (valdez@colpos.mx)

Received: Sep 05, 2024 - Accepted: Sep 14, 2025

Citation: Hernández-Ramos A, Valdez-Lazalde JR, de los Santos-Posadas HM, Reyes-Hernández VJ, López-Serrano PM, Cano-Pineda A, Flores-Magdaleno H (2025). Classification of xeric scrub forest species using machine learning and optical and LiDAR drone data capture. iForest 18: 357-365. - doi: 10.3832/ifor4720-018 [online 2025-12-07]

Communicated by: Francesco Ripullone

Introduction

Arid and semi-arid forest ecosystems are the largest biomes globally (FAO 2019). Despite that, efforts to demonstrate the capabilities of remote sensing technology, particularly drone-mounted spectral or LiDAR sensors, in identifying and classifying plant species are very scarce worldwide (Sankey et al. 2018, Norton et al. 2022, Pervin et al. 2022). Among the main reasons for the limited studies on these ecosystems are their structural complexity and the high diversity of small species. Furthermore, in arid environments, the influence of the soil background on the spectral response can lead to errors such as "same objects with different spectra" or "the same spectrum on different objects", further complicating the accurate identification of species using remote sensing techniques (Gao et al. 2023). This represents a disadvantage for properly developing forest management plans for such a vast global resource.

Sustainable management of any ecosystem plays a fundamental role in preserving its resources, whether timber or non-timber. To achieve this task, it is necessary to rely on accurate information about the ecosystem structure and composition (Mayra et al. 2021, Zhong et al. 2022). Knowing the different species involved, their current range, and the distribution patterns of individuals allows implementing specialized management for each species based on its growth pattern, spatial arrangement (Hell et al. 2022), and resilience to environmental changes (Sivanandam & Lucieer 2022, Qian et al. 2023).

The integration of remote sensing data into a forest vegetation inventory process can result in an efficient and effective classification of tree and shrub individuals of interest, thereby allowing the quantification of the total stock by species in a given area. This is an essential input for sustainable harvest planning of forest raw materials (Zhang & Liu 2013), and could also result in a significant reduction in the investment required for inventory, particularly in large areas. In contrast, the traditional inventory method, based on field sampling, intensive labor, high costs, and a long execution time (Hernández-Ramos et al. 2019) limits its implementation (Qin et al. 2022).

The recent development in aeronautics allows acquiring affordable drones equipped with miniature high-resolution red-green-blue (RGB), multispectral, hyperspectral, and Light Detection and Ranging (LiDAR) remote sensors that can collect information about land surface features in a considerably shorter time than traditional sensors (Yang & Du 2021, Qin et al. 2022). Altogether, these tools effectively describe

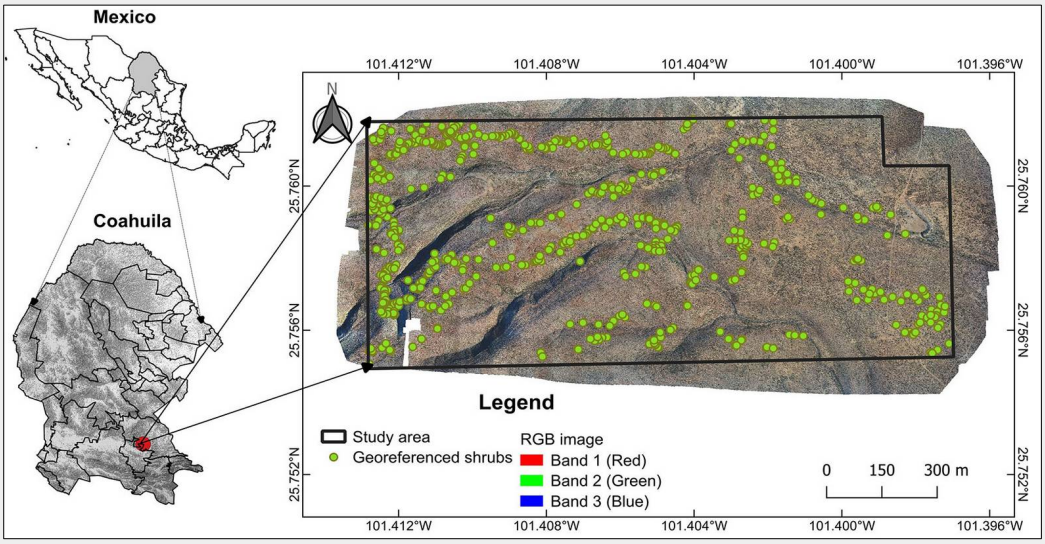

Fig. 1 - Location of the study area. High-resolution RGB image and individual location of shrubland species referenced in the field.

vegetation in horizontal and vertical dimensions, making them valuable for identifying and classifying plant species across various ecosystems. For instance, accurate species classification has been achieved by combining high-resolution LiDAR and drone-acquired optical data (RGB, multispectral, and hyperspectral). This approach has been successfully applied in grasslands (Lu & He 2017, Wang et al. 2023), xeric shrublands with shrub species (Sankey et al. 2018, Pervin et al. 2022, Yue & Li 2023), and forests with tree-like individuals (Sivanandam & Lucieer 2022, Qin et al. 2022, Zhong et al. 2022).

Although drone-based remote sensing data have proven valuable, their high spatial resolution implies the generation of large databases (Lin et al. 2023), which, combined with the presence of diverse vegetative structures, creates a complex scenario that demands efficient methods for accurate analysis (Mayra et al. 2021).

To address the above challenges, machine learning and deep learning have become essential tools for processing and analyzing such data (Cao et al. 2018, Qin et al. 2022). Notable machine-learning algorithms include Gradient Boosting Machines (GBMs), Classification and Regression Trees (CARTs), Random Forests (RFs), and Support Vector Machines (SVMs) (Liu et al. 2017, Norton et al. 2022, Lin et al. 2023). In deep learning, algorithms such as YOLO, Faster R-CNN, and RetinaNet have shown promising results in species classification based on combinations of RGB, multispectral, hyperspectral, and LiDAR remote sensing data (Beloiu et al. 2023, Huang et al. 2024). Despite these advances, few studies have demonstrated the effectiveness of these technologies in species classification within arid and semi-arid ecosystems. Valuable contributions in this area include the studies by Sankey et al. (2018), Tang et al. (2022), Pervin et al. (2022), Norton et al. (2022), and Wang et al. (2023).

This study aimed to identify and classify xeric scrub species from arid and semi-arid regions using a combination of multispectral, RGB, and LiDAR remote sensing data collected by drones. The underlying hypothesis is that the structural variability of a xeric shrubland can be captured in optical and LIDAR variables, thereby enabling the identification of non-timber forest species growing in these ecosystems.

Materials and methods

The study area is located within the Ejido Hipólito, Ramos Arizpe Municipality, Coahuila, Mexico (25.756° N, 101.408° W; WGS84 – Fig. 1), covering 116 ha, with altitudes ranging from 1134 to 1249 m a.s.l. and an average slope of 16%. The climate is arid/semi-warm (BSohw), with a precipitation range of 125-300 mm per year and average temperatures of 9-28 °C. The vegetation corresponds to rosetophilous desert scrub under current forest management, dominated by shrubs such as *Agave lechuguilla* Torr. (Lechuguilla), *Euphorbia antisyphilitica* Zucc. (Candelilla), *Jatropha dioica* Cerv. (Sangre de Drago), *Larrea tridentata* (Sessé & Moc. ex DC.) (Gobernadora), *Hechtia glomerata* Zucc. (Guapilla), *Opuntia spp*. (Nopal), and trees such as *Vachellia farnesiana* (L.) Willd. (Huizache) and *Neltuma glandulosa* Torr. (Mezquite).

Field data capture and processing

Field surveys were carried out to generate a georeferenced database of 343 plant specimens using a Garmin eTrex® GPS receiver (error ± 3.0 m). Additionally, 303 individuals were identified in the RGB imagery. Sampling was focused on plants with clear and distinctive structures to minimize misidentification with other species. Efforts were made to ensure a homogeneous and spatially dispersed distribution of sampling points across the study area, reflecting species distribution patterns and capturing landscape variability. Overall, the geographic coordinates (latitude and longitude) of 646 individuals were recorded and used for algorithm training (Fig. 1). The GPS coordinates were geometrically corrected to UTM zone 14, WGS84, based on the RGB images.

For the analysis, individual coordinates were organized by species, focusing on the highest-density species: *A. lechuguilla* (101 specimens), *E. antisyphilitica* (150), and *L. tridentata* (92). Additionally, morphologically similar species were grouped into shrub categories, such as opuntias (50 specimens), which included *Opuntia rastrera* Weber, *O. engelmannii* subsp. *Lindheimeri, Cylindropuntia leptocaulis* (DC.) F. M. Knuth, *C. imbricata* (Haw.) F.M.Knuth; palms (36 specimens), including *Yucca filifera* Chabaud, *Y. treculeana* Carrière, *Dasylirion cedrosanum* Trel.; trees (44 specimens), including *V. farnesiana, Senegalia berlandieri* Britton & Rose, *V. rigidula* Benth., *N. glandulosa*; and shrubs (173 specimens), comprising all remaining species not classified into previous groups.

Remote sensing data and processing

Multispectral imaging

A DJI Phantom 4M multirotor drone flight was conducted, equipped with a five-band multispectral camera: blue (B_S, 450 nm), green (G_S, 560 nm), red (R_S, 650 nm), Red-Edge (RE, 730 nm), and near-infrared (NIR, 840 nm). The images were taken at a height of 150 m, with a spatial resolution of 0.10 m, and were georeferenced using an RTK module (Real Time Kinematic) to a UTM zone 14, WGS84 coordinate system (Fig. 2b, Fig. 2f). The orthomosaic, radiometric calibration, and atmospheric correction were all automatically executed in DJI Terra v. 3.8.0.

RGB and LiDAR imaging

The area was also scrutinized with a DJI Matrice 300 RTK drone, a Zenmuse L1 sensor, and an RGB camera (20 MP – Fig. 2d). The flight altitude was 180 m, with 75% overlap. The RGB images resulted in a spatial resolution of 0.04 m and three bands (red [R_{rgb}], green [G_{rgb}], and blue [B_{rgb}]), from which hue values were obtained (Fig.

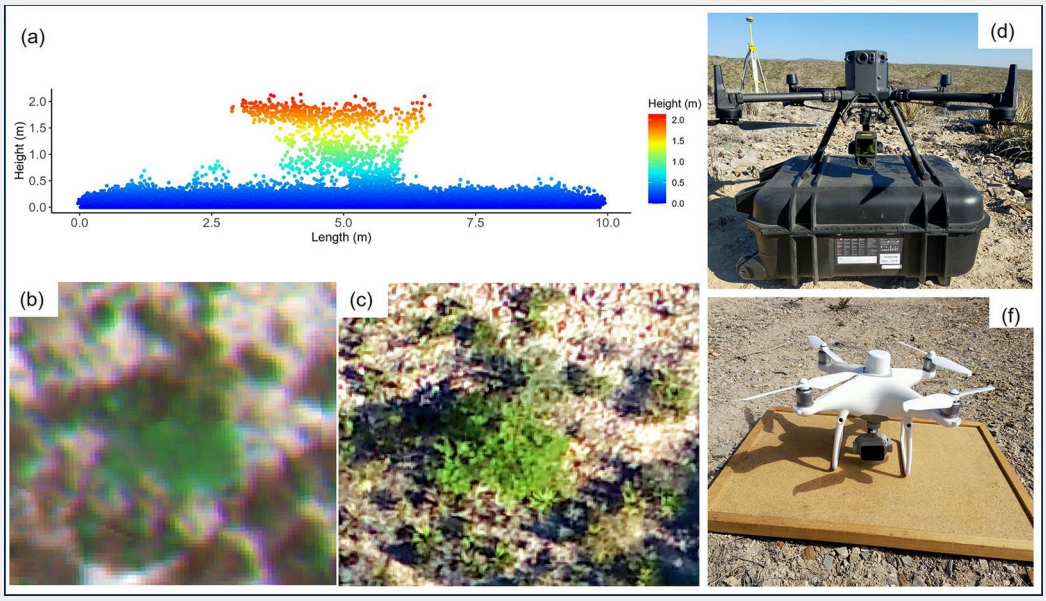

Fig. 2 - Remotely sensed view of shrub species. LiDAR point cloud (a), multispectral image (b), and RGB image (c). Data acquisition equipment: DJI Matrice 300 RTK with Zenmuse L1 (d) and DJI Phantom 4M (f).

2c). The LiDAR point cloud consisted of two returns and an average density of 193.62 points m^{-2} (Fig. 2a). Both items were orthorectified by RTK to the UTM zone 14 coordinate system, WGS84. The drone-captured data were processed in RStudio (R Core Team 2022), using the procedures and methods implemented in the "lidR" packages (Roussel et al. 2020) for LiDAR and in the "GLCMTextures" (Hall-Beyer 2017) package for the extraction of spectral-texture and RGB metrics.

LiDAR-based individual bush extraction

To detect shrubby individuals, the LiDAR point cloud was pre-processed as follows: (i) extreme points (outside the frequency distribution of the maximum and minimum altitudes of the study area) were eliminated by means of altitude filtering (Fig. S1a in Supplementary material); (ii) points were classified into ground and non-ground (vegetation) through the Progressive Morphological Filtering (PMF) procedure (Zhang et al. 2003) using a window size of 0.9 m and a height threshold of 0.03 m, which corresponds to the minimum height of existing vegetation (Fig. S1b); (iii) a 0.5 m spatial resolution Digital Elevation Model (DEM) was generated from points classified as ground using the K-nearest neighbor (K-NN) and the Inverse Distance Weighting (IDW) interpolation algorithms; and (iv) the point cloud was normalized by subtracting the DEM to the Z-coordinate (altitude) of each point classified as non-ground. This eliminates the influence of DEM on shrub height (Silva et al. 2022 – Fig. S1c).

A 1.5 m-diameter circular sampling window and a minimum cut-off height of 0.05 m were used to detect the highest points corresponding to each shrub in the zone using the normalized cloud and the Local Maximum Filter (LMF) algorithm (Mayra et al. 2021, Qin et al. 2022). The point cloud was then segmented using the Dalponte-2016 algorithm (Dalponte & Coomes 2016). This algorithm used the LMF parameters to group and assign a unique identifier to the points that make up each individually segmented shrub. This allowed to accurately measure each shrub in the field and simplify the calculation of height and intensity metrics.

Extraction and selection of optic and LiDAR metrics

To represent the variability of structures and conditions of arid and semi-arid vegetation, 143 metrics were calculated from LiDAR (57), spectral (54), and RGB (32) data. The latter include the B_S, G_S, R_S, RE, and NIR spectral (S) bands, and the color levels (RGB = 0-255) R_{rgb}, G_{rgb}, and B_{rgb}. To reduce the effect of saturation on image values,

Tab. 1 - List of vegetation structure metrics calculated from the segmented LiDAR point cloud for each detected shrub individual.

Attribute	Code	Description	Attribute	Code	Description
Point cloud	n	Number of points	Intensity	itot	Sum of intensities for each return
	area	Individual area (m^2)		imax	Maximum intensity
Normalized Z	zmax	Maximum height (m)		imean	Mean intensity
	zmean	Mean height (m)		isd	Standard deviation of intensity
	zsd	Standard deviation of height		iskew	Skewness of intensity
	zskew	Skewness of height		ikurt	Kurtosis of intensity
	zkurt	Kurtosis of height		ipground	Intensity returned by points classified as "ground" (%)
	zentropy	Entropy of height		ipcmzqx	Intensity returned below the k-percentile of height (%)
	pzabovezmean	returns above zmean (%)		ipxth	Intensity returned by 1^{st}, 2^{nd}, 3^{rd},x^{th}, returns (%)
	pzabovex	Returns above the x percentile (%)	Point cloud	n	Number of points
	zqx	Quantile of height		area	Individual area (m^2)
	zpcumx	Cumulative returns per individual (%)	Classification	pground	Returns classified as "ground" (%)

eight texture metrics per band were included, derived from the Gray Level Co-occurrence Matrix (GLCM), which are: mean (Me), variance (Va), correlation (Co), entropy (En), second moment (Sm), homogeneity (Ho), contrast (Con) and dissimilarity (Di) (Hall-Beyer 2017).

Additionally, 14 vegetation indices (VIs) were included to mitigate the effect of soil albedo on vegetation reflectance and to highlight variations across different cover types. The NDVI, RVI, DVI, SAVI, MSAVI, GCI, GDVI, GRVI, and GNDVI indices were generated from spectral data, and the GRVI, RGBVI, GLI, VARI, and NGRDI indices from RGB images (Naji 2018, Flores-Rodríguez et al. 2020, Hurtado & Lizarazo 2022, Qin et al. 2022 – see Tab. S1 in Supplementary material).

The LiDAR metrics were extracted from the normalized segmented cloud to use the specific records of each detected individual. For this, the normalized Z attributes (Height, m – Silva et al. 2022), the intensity, and the classification of points (Cao et al. 2018) were used. The extraction was performed by deriving standard metrics at different levels of regularization using the "stdmetrics" function in the "lidR" package (Lucas et al. 2019, Tab. 1). The altitude (m) of each individual was also obtained from the LiDAR-generated DEM.

Including diverse variables in the modeling process can lead to redundant information, thus affecting classification accuracy (Cao et al. 2018). To avoid redundancy, we used the Random Forests with Boruta (RFB) and the Xtreme Gradient Boosting (XGB) algorithms to select relevant variables. RFB uses random permutations to choose variables that significantly (α=0.05) contribute to an increased accuracy (Kursa & Rudnicki 2010). XGB evaluates the increase in node purity using the Gini coefficient, which serves as a unit of measurement for estimating prediction variance (James et al. 2023). In both cases, variables with a positive and significant importance value were selected.

Statistical analysis

Six machine learning algorithms were evaluated to classify shrub individuals. All algorithms were adjusted using ensemble models to increase accuracy. Boosting was used for AdaBoost (adaptive boosting, AB), GBM, and XGB; Bagging for CART, RF, and SVM. In the latter, a Gaussian Kernel was used to achieve appropriate adjustments when working with a high number of variables (Kowalczyk 2017). Optimal hyperparameters for the models were determined *via* cross-validation with 5 to 10 iterations. All algorithms were performed in the RStudio "caret" package (Kuhn 2008).

The algorithms were trained and evaluated in two phases. First, the models were adjusted with two selection approaches (RFB and XGB) and with all the variables generated from the spectral data, RGB, and LiDAR; for both selection approaches, the best algorithms, as well as the set of variables (metrics) with the most significant contribution to the classification, were selected. In the second phase, the algorithms with the best statistics were adjusted using the chosen set of variables to evaluate the capacity of the different types of data, used individually and combined, to classify shrub vegetation in arid and semi-arid ecosystems.

Seventy percent of the field data was used to train the algorithms, and the remaining 30% was used as a test set. The models' fit was assessed using bias and agreement measures derived from each algorithm's confusion matrix: overall training accuracy (TA), overall test accuracy (OTA), the Kappa coefficient (K), and specific accuracy per classification group (SA). In addition, the importance of the variables in the classification was assessed with the Gini coefficient (James et al. 2023).

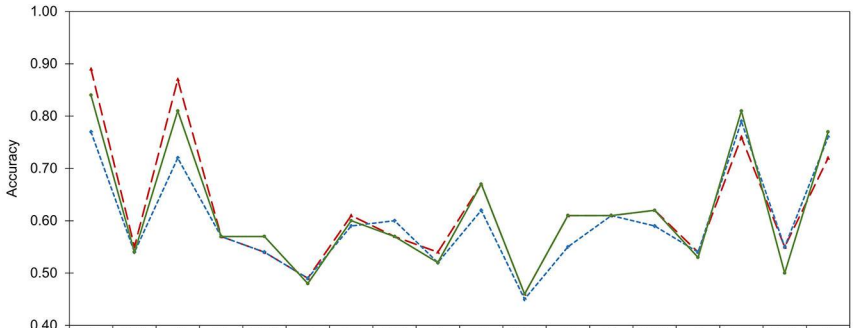

	TA	OTA	K	TA	OTA	K	TA	OTA	K	TA	OTA	K	TA	OTA	K	TA	OTA	K
	AB			GBM			XGB			CART			RF			SVM		
RFB	0.89	0.55	0.87	0.57	0.54	0.49	0.61	0.57	0.54	0.67	0.46	0.61	0.61	0.62	0.54	0.76	0.55	0.72
XGB	0.77	0.54	0.72	0.57	0.54	0.49	0.59	0.60	0.52	0.62	0.45	0.55	0.61	0.59	0.54	0.79	0.55	0.76
All	0.84	0.54	0.81	0.57	0.57	0.48	0.60	0.57	0.52	0.67	0.46	0.61	0.61	0.62	0.53	0.81	0.50	0.77

Fig. 3 - Accuracy of algorithms and variable selection methods for the classification of xerophytic shrub species. (TA): overall training accuracy; (OTA): overall test accuracy; (K): Kappa coefficient; (AB): adaptive boosting; (GBM): gradient boosting machine; (XGB): Xtreme gradient boosting; (CART): classification and regression trees; (RF): Random Forest; (SVM): support vector machines.

Results

Individual bush segmentation

The identification of individuals derived from the LiDAR cloud revealed a total of 471,625 shrubs of all species associated with xerophytic scrub in the study area. These presented an average individual shrub cover of 0.232 m² (range: 0.0094-12.223 m²) and an average height of 0.342 m (range: 0.05-6.63 m). The individuals' geographic locations showed an average spatial error of 0.40 m relative to the multispectral image, attributable to differences in acquisition equipment. This mismatch was rectified by a geometric correction of the multispectral image from the RGB orthomosaic (see Fig. S2 in Supplementary material).

Selection of metrics and algorithm evaluation

The 143 spectral, RGB, and LiDAR metrics were extracted for each individual detected in the point cloud (471,625 shrubs) and for the sampled individuals (646 shrubs). Five metrics related to the percentage of return intensity (ipxth) were excluded because they lacked values, leaving 138 metrics. The selection of variables with RFB was reduced to 102 metrics (LiDAR: 35, spectral: 43, and RGB: 24), whereas XGB selected only 32 (LiDAR: 13, spectral: 12, and RGB: 7). Regarding the efficiency of the variable sets, RFB (TA: 0.70, OTA: 0.55, K: 0.64) and without selection (TA: 0.70, OTA: 0.54, K: 0.63) presented the highest accuracy. In contrast, XGB had lower accuracy (TA: 0.67, OTA: 0.55, K: 0.61), due to its strict discrimination, which could eliminate essential variables for a specific class of shrubs (Fig. 3).

Of the selected variables, the most relevant in the classification of shrubs were Altitude, NIR, R_{rgb}_Me, RE, and GDVI, for the RFB method (Fig. 4a); and R_s, Altitude, RE_Va, RE, NIR, and itot with XGB (Fig. 4b). In general, spectral and RGB images presented a greater number of variables with significance in both methods, in addition to their texture and VI derivatives. For LiDAR, the reduction was greater, which implies a lesser contribution (Fig. 4). With these sets of variables (RFB, XGB, and without selection), the AB, GBM, XGB, CART, RF, and SVM algorithms were evaluated, in which the overall mean TA was 0.69, OTA was 0.54, and K was 0.63. The highest values of TA and K were presented in AB (0.83 and 0.80, respectively), SVM (0.79 and 0.75), and CART (0.65 and 0.59); whereas the lowest were in GBM (0.57 and 0.49 – Fig. 3).

As for OTA, the best models were RF (0.61), XGB (0.58), and GBM (0.55), whereas the rest showed a drop in OTA relative to TA, suggesting overfitting and the inability to predict new observations accurately. In this parameter, CART (0.46) had the lowest fit (Fig. 3). The algorithms that performed best in bush classification were AB,

SVM, and RF. The first two were chosen for their ability to fit the training data, while the last one stood out for its statistical stability and higher prediction accuracy (OTA). Using these three best-fitting algorithms and the set of metrics generated with RFB, which was superior, the remote sensing data types were evaluated for species and shrub class classification.

Spectral, RGB, and LiDAR data assessment

Across all data combinations, the AB and SVM algorithms achieved the highest average training accuracy (TA: 0.74 and 0.68, K: 0.69 and 0.62, respectively). However, prediction in the OTA is low (0.44 and 0.46) (Tab. 2), which means overfitting and a low efficiency to perform new estimations. On the contrary, although RF obtained lower training values for TA and K, its accuracy was higher in the test set (OTA: 0.49), in addition to show stability in the learning and prediction process (Tab. 2). Therefore, the RF model was selected for the assessment of LiDAR, spectral, and RGB data.

When the predictive power (OTA) of different types of remote sensing data for shrub species classification was compared, spectral data showed the highest accuracy (0.43), followed by RGB (0.42) and LiDAR metrics (0.33). The combination of two types of data increased the classification accuracy in all cases (Tab. 2). The data set composed of LiDAR and spectral data was superior (0.52), with an increase of 20.93%, 23.81% and 57.58% compared to the independent use of spectral, RGB, and LiDAR variables, respectively. Finally, combining all three data types (0.62) yielded an accuracy gain of 19.23%, suggesting that using all variables together improves the classification of species and shrub classes.

Classification of shrub species and classes

The RF algorithm was trained to classify shrub species and groups using 646 individuals and a combination of three types of selected and refined remote sensing data. The overall accuracy was 0.64 (range: 0.60-0.68), and the Kappa index was 0.56. The minimum specific accuracy (SA) achieved for the classes was 0.55. The values for each species and shrub group were 0.73 (*E. antisyphilitica*), 0.70 (opuntias), 0.67 (palms), 0.65 (*L. tridentata*), 0.59 (trees and shrubs), and 0.55 (*A. lechuguilla*).

Spectral data made a greater contribution to species and shrub group classification, as they provided more variables. Among the 20 variables with the highest importance, spectral data contributed with 10 metrics to the shrub classification (NIR, DVI, R_S, RE, GDVI, SAVI, NIR_Va, MSAVI, G_S, B_S), compared to eight metrics extracted from LiDAR (Altitude, zmean, zq95, zq85, zmax, zq65, zsd, zq80) and two metrics from the RGB image (R_{rgb}_Me, G_{rgb}_Me – Fig. S3 in Supplementary material). Of all metrics, altitude made the most significant contribution, followed by a group of spectral variables (bands and VI NIR, DVI, R_S, RE, GDVI). Texture metrics from RGB data had less influence on species discrimination.

The results of the classification of the 471,625 shrubs detected with LiDAR are shown in Tab. 3. Adequate classifications were obtained for *E. antisyphilitica* and *L. tridentata*, as well as for the group of trees, opuntias, and palms. Field density and spatial distribution were obtained according to model estimates (Fig. 5). However, a low precision was observed when classifying *A. lechuguilla* (one of the most abundant species in the study area), despite having a good number of samples for fitting the model, so an underestimation of this spe-

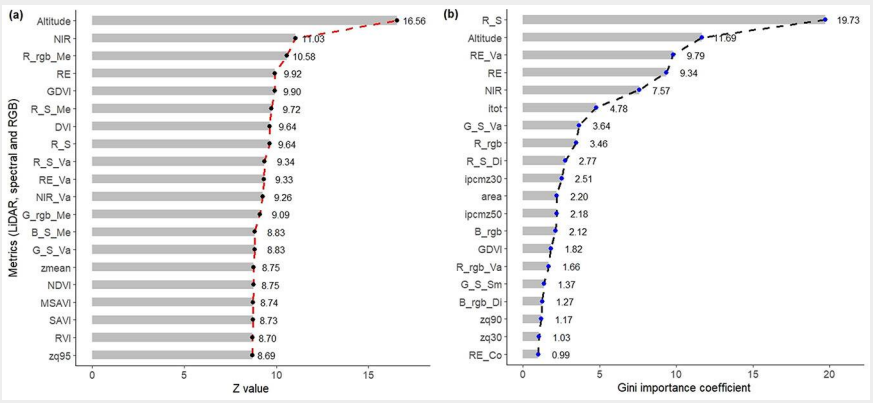

Fig. 4 - Selected spectral, RGB, and LiDAR metrics with (a) Random Forests with Boruta (RFB), and (b) extreme gradient boost (XGB) with greater significance in the classification of xerophytic shrubland species. (R): red; (G): green; (B): blue; (S): spectral data; (rgb): RGB data; (Me): mean; (Va): variance; (Di): dissimilarity; (Sm): second moment.

Tab. 2 - Accuracy of the three selected models using spectral, RGB, and LiDAR data individually and combined for the classification of species and shrub groups of a xeric shrubland. (RFB): Random forests with Boruta; (AB): Adaptive boosting; (RF): Random forests; (SVM): Support vector machines; (TA): overall training accuracy; (OTA): overall test accuracy; (K): Kappa coefficient; (L): LiDAR; (S): spectral; (RGB): red-green-blue image.

Selection	Data	AB			RF			SVM		
		TA	OTA	K	TA	OTA	K	TA	OTA	K
RFB	L	0.67	0.34	0.61	0.42	0.33	0.32	0.58	0.35	0.49
	S	0.63	0.39	0.55	0.47	0.43	0.37	0.65	0.42	0.58
	RGB	0.67	0.39	0.60	0.42	0.42	0.30	0.61	0.40	0.53
	L-S	0.74	0.45	0.69	0.54	0.52	0.45	0.70	0.51	0.64
	L-RGB	0.78	0.43	0.74	0.53	0.49	0.43	0.68	0.49	0.62
	S-RGB	0.79	0.45	0.75	0.51	0.51	0.42	0.70	0.51	0.65
	L-S-RGB	0.89	0.55	0.87	0.61	0.62	0.54	0.76	0.55	0.72
-	*Mean*	*0.74*	*0.44*	*0.69*	*0.51*	*0.49*	*0.42*	*0.68*	*0.46*	*0.62*

Tab. 3 - Classification parameters of shrubs detected with the LiDAR point cloud in the study area and average dimensionality values.

Species/Category	Training Individuals (n)	Classified individuals (n)	Classified individuals (%)	Mean height (m)	Mean coverage (m^2)
A. lechuguilla	101	46,272	9.8	0.265	0.229
Trees	44	1,897	0.4	1.183	0.530
Shrubs	173	251,161	53.3	0.334	0.230
E. antisyphilitica	150	120,404	25.5	0.271	0.230
L. tridentata	92	43,693	9.3	0.549	0.229
Opuntias	50	5,326	1.1	0.542	0.231
Palms	36	2,872	0.6	1.091	0.425

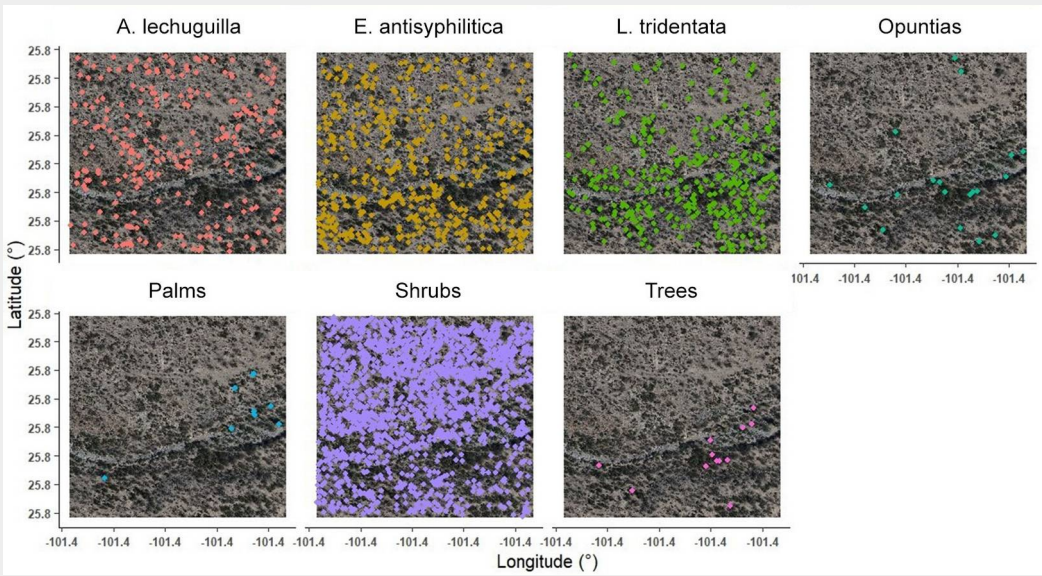

Fig. 5 - Classification of individuals by shrub species and groups of a xerophytic shrubland obtained from remote sensing data and the Random Forest model.

cies is assumed. This may be because the spectral response of *A. lechuguilla* could have been confused with that of other species in the shrub class. In fact, distinguishing it from similar species can be difficult due to its agglomerated growth form (Sankey et al. 2017, Norton et al. 2022).

The classified species and groups presented coverages of 0.557 m² for trees, 0.231 m² for shrubs, 0.230 m² for opuntias, 0.408 m² for palms, 0.230 m² for *E. antisyphilitica*, 0.228 m² for *L. tridentata,* and 0.229 m² for *A. lechuguilla.* The highest height was registered in the tree group (1.18 m, range; 0.30-5.13 m), followed by the palms (1.09 m, range: 0.32-4.50 m), whereas the rest were distributed between average heights ranging from 0.25 m to 0.55 m (Tab. 3). Regarding this variable, overestimates were found in all classes, especially for *E. antisyphilitica* and *A. lechuguilla* with maximum heights of 4.81 m and 4.03 m, respectively, values that are outside the expected growth interval of these species.

Discussion

Individual shrub segmentation

In this study, LiDAR data and the FML algorithm were used to segment individual plants based on vegetation structural dimensions, yielding accurate results validated against RGB images (Fig. S2 in Supplementary material). These findings are consistent with recent studies on individual tree detection (Wu et al. 2019, Mayra et al. 2021, Qin et al. 2022), although with lower accuracy for shrubs. This reduced accuracy is attributed to the morphological diversity of vegetation in arid and semi-arid ecosystems, which includes spherical, cylindrical, and rectangular shapes (Liu et al. 2022). Furthermore, in areas with high species density, both underestimation of individual counts and overestimation (false individuals) in bare soil areas associated with rocky bodies were observed.

The bias generated in the detection of individuals is attributed to the similarity in the vegetation height. This was observed during maximum Z-value filtering, where only larger individuals were identified, and the smaller ones were eliminated, making it difficult to separate individual shrubs and leading to individual loss during LiDAR scanning. Sankey et al. (2017) mentioned that accuracy in this process is highly dependent on the quality of cloud segmentation, which is influenced by point density, number of bounces, structural similarity, and species agglomeration. In addition, using fixed parameters to identify all species or plant strata can increase detection errors, particularly for shrub species (Dashti et al. 2019).

Using vegetation-based parameters improved the detection of individuals. This is supported by recent findings of Wu et al. (2019) and Xu et al. (2023), who used small windows and a minimum cut-off height to generate a higher number of individuals in shrub or small vegetation. In particular, the cut-off height is crucial for detecting individuals. It should be comparable to the minimum vegetation height to capture the variability in shrub and tree structures (Pervin et al. 2022). In addition, it is recommended to adopt a short cut-off height, according to the flattened shape of the shrub canopy, as described by Qian et al. (2023).

Selection of metrics and algorithm evaluation

A crucial step in the training process is variable selection, which helps eliminate multicollinearity and less important variables, thereby improving the accuracy and performance of algorithms in classification and regression (Lin et al. 2023). In this study, 138 remotely sensed metrics were employed to characterize three species and seven shrub groups in a xerophytic rosetophytic shrubland. Two variable selection techniques were applied, RFB and XGB, which reduced the metrics by 26.10% and 76.81%. The first was selected to avoid omitting important information during classification. This is also recommended for modeling complex structures, such as vegetation in arid and semi-arid ecosystems, where a large set of variables is needed to achieve species discrimination with low estimation bias (Cao et al. 2018, Lin et al. 2023). In addition, several studies highlight the integration of remote sensing data to improve classification accuracy and detail (Norton et al. 2022, Wang et al. 2023). In this case, precision increased by 3.3% by eliminating correlated or redundant variables. This improvement has been corroborated in similar studies, which demonstrated that optimal variable selection can improve the accuracy of species classification. This finding applies to both shrubby species in arid and semi-arid regions (Yang & Du 2021, Norton et al. 2022, Pervin et al. 2022, Tang et al. 2022) and arboreal species in temperate and tropical forests (Dashti et al. 2019, Lin et al. 2023).

Evaluation of spectral, RGB, and LiDAR data

The effectiveness of integrating data from multiple remote sensors for classifying plant species across various ecosystems has already been documented. The best results have been obtained by combining metrics derived from LiDAR and optical imaging (spectral and RGB – Norton et al. 2022, Zhong et al. 2022, Lin et al. 2023). In this work, integrating optical and LiDAR remote sensing data increased the classification accuracy of shrub species by 23.80%, with OTA rising from 0.42 when used individually to 0.52 when combining the three data types, which aligns with previous findings. As reported by Qian et al. (2023), the inclusion of vegetation structure metrics (LiDAR) improves the estimates by describing the dimensions of plant species, and by complementing the optical information for a complete characterization of vegetation (Cao et al. 2018, Zhong et al. 2022). The in-

dividual use of these data limits the ability to describe vegetation properties, as variables are captured separately along a single dimension (Qin et al. 2022, Lin et al. 2023). Therefore, it is necessary to incorporate various types of remotely sensed data to achieve a comprehensive characterization of vegetation, covering both its vertical and horizontal aspects.

Data derived from multispectral images yielded the best results, which agree with similar research on classifying shrubby individuals from other arid and semi-arid regions (Sankey et al. 2017, Sankey et al. 2018, Mayra et al. 2021, Qin et al. 2022). This is because the spectral signatures of the species can be discriminated, along with the high spatial resolution of the spectral and RGB images (0.10 m). Although LiDAR did not perform well in species classification, it was indispensable for improving the results.

Nonetheless, this result differs from the findings reported by Liu et al. (2017) and Cao et al. (2018), who observed better performance with LiDAR metrics than with optical data. This can be attributed to the fact that these authors modelled the tree structures of coniferous forests, in which the crown spectral response is similar, and the most relevant differences lie in the arrangement of branches and crown morphometry, aspects better represented by structure-derived LiDAR variables. Moreover, Zhong et al. (2022) noted that differences in the efficiency of different types of remote sensing data are attributable to the capture season and sensor type, as well as to the complexity of the evaluated phenomenon and the classification algorithm used.

Classification of shrub species and classes

Our results align with similar studies that used the RF machine learning algorithm to classify shrub species in arid and semi-arid regions. Although RF did not achieve the highest training accuracy, it demonstrated superior prediction performance compared to the SVM and AB algorithms (Cao et al. 2018, Norton et al. 2022, Qin et al. 2022). These results align with other studies that compare several classification algorithms, showing that RF achieves higher prediction accuracy than SVM, AB, CART, and GBM (Liu et al. 2017, Lin et al. 2023). This success is attributed to RF's flexible nature as a learning algorithm, especially its ability to effectively handle large datasets (Immitzer et al. 2012). RF divides the data into adaptive sections (*i.e.*, trees), and fits a model specifically for each classification group. This adaptive approach has proven fundamental for obtaining accurate results (Sankey et al. 2018, Pervin et al. 2022). In contrast, Mayra et al. (2021) showed that, when classifying tree species in a mixed temperate forest, decision tree-based methods (GBM and RF) had significant difficulties in separating deciduous species, which was attributed to the spatial incompatibility of field and remotely sensed data, affecting the spectral signature of species.

On the other hand, classification accuracies in this study ranged from 0.55 to 0.73 at the species level, and an overall accuracy of 0.64. The accuracy levels may have been influenced by factors such as the amount of data available per species and shrub class, as well as the distinct characteristics of each species. Additionally, the species density imbalance in the study area could have contributed to these results. In this regard, Huang et al. (2024) demonstrated that classification accuracy in arid grasslands varied with sample size per class, reporting accuracies of 0.78-0.90, which are higher than those found in this study. Similarly, Norton et al. (2022) achieved accuracies of 0.86-0.98 when classifying five tree species in semi-arid ecosystems, while Liu et al. (2022) obtained accuracies of 0.70-0.82 using a combination of remote sensing data (LiDAR, multispectral, and RGB) to improve classification precision.

Although these technologies offer promising advances in species classification and environmental monitoring, they still face significant challenges, including issues with data quality and ongoing improvement needs. Addressing these limitations is critical to fully realizing the potential of drone-borne remote sensing in non-timber forest management.

Conclusions

This study demonstrates the potential of combining high-resolution multispectral, RGB, and LiDAR data acquired with drone-borne sensors with machine learning algorithms for classifying xeric scrub vegetation in arid and semi-arid ecosystems. Combining LiDAR structural information with optical data (multispectral and RGB), the proposed approach achieved a 19.23% improvement in classification accuracy compared to the individual data sources. This multidimensional strategy enabled not only the detection and spatial mapping of over 471,625 individual shrubs using LiDAR point clouds, but also the successful identification of non-timber forest species with moderate to high accuracy. The results emphasize the relevance of spectral variables in distinguishing among species and highlight the critical role of LiDAR in capturing vegetation structure, particularly vertical complexity.

These findings highlight the value of drone-based remote sensing combined with machine learning algorithms as a novel, scalable, and cost-effective framework for precision forest management in data-scarce arid and semi-arid ecosystems.

Future applications of this approach may include monitoring vegetation dynamics, assessing biodiversity, and informing restoration strategies, thereby contributing to the sustainable management of dryland forest resources.

Acknowledgments

The first author thanks the *Secretaría de Ciencia, Humanidades, Tecnología e Innovación* (SECIHTI) for the scholarship granted to pursue his doctoral studies in Forest Sciences at the *Colegio de Postgraduados*. We would also like to thank the *Instituto Nacional de Investigaciones Forestales, Agrícolas y Pecuarias* (INIFAP) for funding the project "Estimation of forest variables in arid and semi-arid ecosystems using remote sensing data for the use of non-timber forest resources", through which the field data were collected.

Conflicts of Interest

The authors declare no conflict of interest.

References

Beloiu M, Heinzmann L, Rehush N, Gessler A, Griess VC (2023). Individual tree-crown detection and species identification in heterogeneous forests using aerial RGB imagery and deep learning. Remote Sensing 15 (5): 1463. - doi: 10.3390/rs15051463

Cao L, Pan J, Li R, Li J, Li Z (2018). Integrating airborne LiDAR and optical data to estimate forest aboveground biomass in arid and semi-arid regions of China. Remote Sensing 10: 532. - doi: 10.3390/rs10040532

Dalponte M, Coomes DA (2016). Tree-centric mapping of forest carbon density from airborne laser scanning and hyperspectral data. Methods in Ecology and Evolution 7: 1236-1245. - doi: 10.1111/2041-210X.12575

Dashti H, Poley A, Glenn NF, Llangakoon N, Spaete L, Roberts D, Enterkine J, Flores AN, Ustin SL, Mitchell JJ (2019). Regional scale dryland vegetation classification with an integrated LiDAR-hyperspectral approach. Remote Sensing 11: 2141. - doi: 10.3390/rs11182141

FAO (2019). Trees, forests and land use in drylands: the first global assessment. Forestry Paper, Food and Agriculture Organization - FAO, Rome, Italy, pp. 184. [online] URL: http://openknowledge.fao.org/handle/20.500.14283/ca7148en

Flores-Rodríguez AG, Flores-Garnica JG, González-Eguiarte DR, Gallegos-Rodríguez A, Zarazúa-Villaseñor P, Mena-Munguía S (2020). Revisión de métodos de sensores remotos para la detección y evaluación de la severidad de incendios forestales [Review of remote sensing methods for the detection and evaluation of the severity of forest fires]. Gestión y Ambiente 23 (2): 273-283. [in Spanish] - doi: 10.15446/ga.v23n2.93682

Gao X, Hao F, Pi W, Zhu X, Zhang T, Bi Y, Zhang Y (2023). Identification and classification of degradation-indicator grass species in a desertified steppe based on HSI-UAV. Spectroscopy 38 (11): 14-20. - doi: 10.56530/spectroscopy.dr5881c1

Hall-Beyer M (2017). Practical guidelines for choosing GLCM textures to use in landscape classification tasks over a range of moderate spatial scales. International Journal of Remote Sensing 38 (5): 1312-1338. - doi: 10.1080/01431161.2016.1278314

Hell M, Brandmeler M, Briechle S, Krzystek P (2022). Classification of tree species and stand-

ing dead trees with LiDAR point clouds using two Deep Neural Networks: PointCNN and 3DmFV-Net. Journal of Photogrammetry, Remote Sensing and Geoinformation Science 90: 103-121. - doi: 10.1007/s41064-022-00200-4
Hernández-Ramos A, Cano-Pineda A, Flores-López C, Hernández-Ramos J, García-Cuevas X, Martínez-Salvador M, Martínez LA (2019). Modelos para estimar biomasa de *Euphorbia antisyphilitica* Zucc. en seis municipios de Coahuila [Models to estimate biomass of *Euphorbia antisyphilitica* Zucc. in six townships of Coahuila]. Madera y Bosques 25(2): e2521806. [in Spanish] - doi: 10.21829/myb.2019.2521806
Huang Y, Ou B, Meng K, Yang B, Carpenter J, Jung J, Fei S (2024). Tree species classification from UAV canopy images with deep learning models. Remote Sensing 16 (20): 3836. - doi: 10.3390/rs16203836
Hurtado JLA, Lizarazo I (2022). Nuevo índice espectro-temporal para la detección de pérdida forestal en áreas de bosque tropical. Caso de estudio Amazonia colombiana [New Spectro-temporal index for the detection of forest loss in tropical forest areas. A Colombian Amazon case study]. Revista Cartográfica 104: 11-35. [in Spanish] - doi: 10.35424/rcarto.i104.1096
Immitzer M, Atzberger C, Koukal T (2012). Tree species classification with random forest using very high spatial resolution 8-band Worldview-2 satellite data. Remote Sensing 4: 2661-2693. - doi: 10.3390/rs4092661
James G, Witten D, Hastie T, Tibshirani R (2023). An introduction to statistical learning with applications in R. Springer Texts in Statistics, New York, NY, USA, pp. 604.
Kowalczyk A (2017). Support vector machines succinctly. Syncfusion, Inc., Morrisville, NC, USA, pp. 114.
Kuhn M (2008). Building predictive models in R using the caret package. Journal of Statistical Software 28 (5): 28. - doi: 10.18637/jss.v028.i05
Kursa MB, Rudnicki RW (2010). Feature selection with the Boruta Package. Journal of Statistical Software 36: 11. - doi: 10.18637/jss.v036.i11
Lin H, Liu X, Han Z, Cui H, Dian Y (2023). Identification of tree species in forest communities at different altitudes based on multi-source aerial remote sensing data. Applied Sciences 13: 4911. - doi: 10.3390/app13084911
Liu L, Coops NC, Aven NW, Pang Y (2017). Mapping urban tree species using integrated airborne hyperspectral and LiDAR remote sensing data. Remote Sensing of Environment 200: 170-182. - doi: 10.1016/j.rse.2017.08.010
Liu Y, Zhang X, Ma Z, Dong N, Xie D, Li R, Johnston DM, Gao GY, Li Y, Lei Y (2022). Developing a more accurate method for individual plant segmentation of urban tree and shrub communities using LiDAR technology. Landscape Research 48 (3): 313-330. - doi: 10.1080/01426397.2022.2144813
Lu B, He Y (2017). Species classification using Unmanned Aerial Vehicle (UAV)-acquired high spatial resolution imagery in a heterogeneous grassland. ISPRS Journal of Photogrammetry and Remote Sensing 128: 73-85. - doi: 10.1016/j.isprsjprs.2017.03.011
Lucas C, Bouten W, Koma Z, Kissling WD, Seijmonsbergen AC (2019). Identification of linear vegetation elements in a rural landscape using LiDAR point clouds. Remote Sensing 11: 292. - doi: 10.3390/rs11030292
Mayra J, Keski-Saari S, Kivinen S, Tanhuanpaa T, Hurskainen P, Kullberg P, Poikolainen L, Viinikka A, Tuominen S, Kumpula T, Vihervaara P (2021). Tree species classification from airborne hyperspectral and LiDAR data using 3D convolutional neural networks. Remote Sensing of Environment 256: 112322. - doi: 10.1016/j.rse.2021.112322
Naji TAH (2018). Study of vegetation cover distribution using DVI, PVI, WDVI indices with 2D-space plot. Journal of Physics - Conference Series 1003: 012083. - doi: 10.1088/1742-6596/1003/1/012083
Norton CL, Hartfield K, Collins CDH, Leeuwen WJD, Metz LJ (2022). Multi-temporal LiDAR and hyperspectral data fusion for classification of semi-arid woody cover species. Remote Sensing 14: 2896. - doi: 10.3390/rs14122896
Pervin R, Robeson SM, McBean N (2022). Fusion of airborne hyperspectral and LiDAR canopy-height data for estimating fractional cover of tall woody plants, herbaceous vegetation, and other soil cover types in a semi-arid savanna ecosystem. International Journal of Remote Sensing 43 (10): 3890-3926. - doi: 10.1080/01431161.2022.2105176
Qian C, Yao C, Ma H, Xu J, Wang J (2023). Tree species classification using airborne LiDAR data based on individual tree segmentation and shape fitting. Remote Sensing 15: 406. - doi: 10.3390/rs15020406
Qin H, Zhou W, Yao Y, Wang W (2022). Individual tree segmentation and tree species classification in subtropical broadleaf forests using UAV-based LiDAR, hyperspectral, and ultrahigh-resolution RGB data. Remote Sensing of Environment 280: 113143. - doi: 10.1016/j.rse.2022.113143
R Core Team (2022). R: a language and environment for statistical computing. R Foundation for Statistical Computing, Vienna, Austria. [online] URL: http://www.r-project.org/
Roussel JR, Auty D, Coops NC, Tompalski P, Goodbody TRH, Sánchez MA, Bourdon JF, De Boissieu F, Achim A (2020). lidR: an R package for analysis of Airborne Laser Scanning (ALS) data. Remote Sensing of Environment 251: 112061. - doi: 10.1016/j.rse.2020.112061
Sankey T, Donager J, McVay J, Sankey JB (2017). UAV lidar and hyperspectral fusion for forest monitoring in the southwestern USA. Remote Sensing of Environment 195: 30-43. - doi: 10.1016/j.rse.2017.04.007
Sankey TT, McVay J, Swetnam TL, McClaran MP, Heilman P, Nichols M (2018). UAV hyperspectral and lidar data and their fusion for arid and semi-arid land vegetation monitoring. Remote Sensing in Ecology and Conservation 4 (1): 20-33. - doi: 10.1002/rse2.44
Silva CA, Hudak AT, Vierling LA, Valbuena R, Cardil A, Mohan M, Almeyda DRA, Broadbent EN, Almeyda AMZ, Wilkinson B, Sharma A, Drake JB, Medley PB, Vogel JG, Prata GA, Atkins JW, Hamamura C, Johnson DJ, Klauberg C (2022). treetop: a shiny-based application and R package for extracting forest information from LiDAR data for ecologists and conservationists. Methods in Ecology and Evolution 13: 1164-1176. - doi: 10.1111/2041-210X.13830
Sivanandam P, Lucieer A (2022). Tree detection and species classification in a mixed species forest using Unoccupied Aircraft System (UAS) RGB and multispectral imagery. Remote Sensing 14: 4963. - doi: 10.3390/rs14194963
Tang J, Liang J, Yang Y, Zhang S, Hou H, Zhu X (2022). Revealing the structure and composition of the restored vegetation cover in semi-arid mine dumps based on LiDAR and hyperspectral images. Remote Sensing 14: 978. - doi: 10.3390/rs14040978
Wang S, Bi Y, Du J, Zhang T, Gao X, Jin E (2023). The Unmanned Aerial Vehicle (UAV)-based hyperspectral classification of desert grassland plants in Inner Mongolia, China. Applied Sciences 13 (22): 12245. - doi: 10.3390/app132212245
Wu X, Shen X, Cao L, Wang G, Cao F (2019). Assessment of individual tree detection and canopy cover estimation using Unmanned Aerial Vehicle based Light Detection and Ranging (UAV-LiDAR) data in planted forests. Remote Sensing 11: 908. - doi: 10.3390/rs11080908
Xu X, Luricich F, Floriani L (2023). A topology-based approach to individual tree segmentation from airborne LiDAR data. Geoinformatica 27: 759-788. - doi: 10.1007/s10707-023-00487-4
Yang H, Du J (2021). Classification of desert steppe species based on unmanned aerial vehicle hyperspectral remote sensing and continuum removal vegetation indices. Optik 247: 167877. - doi: 10.1016/j.ijleo.2021.167877
Yue K, Li P (2023). The classification characteristics and dynamic changes of desert vegetation based on Unmanned Aerial Vehicle remote sensing. Journal of Biobased Materials and Bioenergy 17 (6): 734-741. - doi: 10.1166/jbmb.2023.2316
Zhang K, Chen S, Whitman D, Shyu M, Yan J, Zhang C (2003). Progressive morphological filter for removing nonground measurements from airborne LiDAR data. IEEE Transactions on Geoscience and Remote Sensing 41 (4): 872-882. - doi: 10.1109/TGRS.2003.810682
Zhang Z, Liu X (2013). Support vector machines for tree species identification using LiDAR-derived structure and intensity variables. Geocarto International 28 (4): 364-378. - doi: 10.1080/10106049.2012.710653
Zhong H, Lin W, Liu H, Ma N, Liu K, Cao R, Wang T, Ren Z (2022). Identification of tree species based on the fusion of UAV hyperspectral image and LiDAR data in a coniferous and broad-leaved mixed forest in Northeast China. Frontiers in Plant Science 13: 964769. - doi: 10.3389/fpls.2022.964769

Supplementary Material

Fig. S1 - LiDAR point cloud processing for shrub detection.

Fig. S2 - Detection of shrubs in a xerophytic shrubland.

Fig. S3 - Significance Gini value of LiDAR, spectral, and RGB metrics in the classification with the Random Forest model (RF) (a). Frequency of classified species and shrub groups (b).

Tab. S1 - Vegetation indices extracted from high-resolution spectral and RGB data obtained with drones.

Link:
Hernandez-Ramos_4720@suppl001.pdf